High-resolution native tandem mass-spectrometry of antibody-drug conjugates and higher order antibody-antigen complexes.

(High-resolution native tandem mass-spectrometry of antibody-based therapeutic constructs)

Andrey Dyachenko[1,2], Guanbo Wang[1,2], Mike Belov[3], Alexander Makarov[1,3], Rob N. de Jong[4], Ewald T.J van den Bremer[4], Paul W.H.I. Parren[4,5], Albert J.R. Heck[1,2].

1. Biomolecular Mass Spectrometry and Proteomics. Bijvoet Centre for Biomolecular Research and Utrecht Institute for Pharmaceutical Sciences, University of Utrecht, Padualaan 8, 3584 CH, Utrecht, The Netherlands.
2. Netherlands Proteomics Center, Padualaan 8, 3584 CH, Utrecht, The Netherlands.
3. ThermoFisher Scientific, Bremen, Germany.
4. Genmab, Utrecht, The Netherlands
5. Department of Immunohematology and Blood Transfusion, Leiden University Medical Center, 2333 ZA Leiden, The Netherlands

Supporting information

Materials and methods

Instrument modifications. Orbitrap Exactive Plus mass spectrometer (Thermo Fisher Scientific, Bremen, Germany) was modified for optimal transmission and detection of ions with m/z up to 50,000[20,21,22] (Figure S1). A dedicated gas line was installed to allow control over the pressure and type of gas introduced into the HCD cell for the more efficient cooling and desolvation of heavy ions. Furthermore, the operating frequency of the front-end RF guides and the HCD cell was lowered to improve ion transmission and diminish the ion loss during activation at high energies; a preamplifier with lower high-pass filter cutoff was used to improve transmission of lower frequency image current signals originating from ions with larger m/z. For ion isolation we used a standard quadrupole mass filter from a Q Exactive™ instrument with a modified electronic board that featured decreased resonance frequency of 284 kHz and an upper mass-selection limit above 20000 m/z.

Materials. Brentuximab vedotin was acquired as a formulated drug from Seattle Genetics (Seattle, WA). The ADC was extracted from these formulation as described earlier[15]. IgG mutants were generated at Genmab (Utrecht, The Netherlands). Peptide-N-Glycosidase F (PNGase F) was purchased from Roche (Manheim, Germany). All other materials were purchased from Sigma Aldrich (Germany).

Generation of non-glycosylated soluble CD38. A codon-optimized construct was generated for the expression of non-glycosylated recombinant His-tagged soluble CD38. PCR was used to amplify the part encoding for the extracellular soluble domain of CD38 from the construct, adding a N-terminal His tag containing six His residues (CD38-ECDHis). Four asparagine amino acids located in specific N-linked

glycosylation recognition sequences were mutated. The construct was cloned in pEE13.4 (Lonza Biologics) and transfected into Freestyle 293-F cells (HEK-293F, Invitrogen). Non-glycosylated CD38-ECDHis was expressed and subsequently purified from cell supernatant using immobilized metal affinity chromatography.

Sample preparation. The extracted ADC brentuximab vedotin was incubated overnight in the presence of PNGase F (1 u per 10 µg of protein) for deglycosylation. The deglycosylated ADC was buffer-exchanged into aqueous ammonium acetate (AmAc, 150 mM, pH 7.5) using Amicon Ultra centrifugal filter units (Merck Millipore) with 10kDa MWCO and the sample concentration was adjusted to 5 µM prior to analysis. For partial disulfide bond reduction, the ADC was incubated with 2mM of dithiothreitol (DTT) for 30 minutes and analyzed directly afterwards. IgG1 and non-glycosylated CD38 were buffer-exchanged using Amicon Ultra centrifugal filter units (Merck Millipore) with 10kDa MWCO.

Quadrupole ion transmission calculations. The ion transmission through quadrupole was calculated based on the RawOvFtT factor value that is stored for each scan in the Thermo .RAW file format. The RawOvFtT factor describes ion count (IC) in the Orbitrap FT cell. The IC corresponding to the peak of interest in the full scan mode is calculated as a fraction of the total IC (eq S1). The ion transmission is the ratio between this value and the IC in the isolation mode (eq. S2).

$$IC_{Full}^{i} = IC_{Full}\frac{I_i}{I_\Sigma} \qquad \text{(S1)}$$

$$IT = \frac{IC_{iso}^{i}}{IC_{Full}^{i}} \qquad \text{(S2)}$$

where IC_{Full}^{i} and IC_{iso}^{i} are the ion count values corresponding to *i* peak in the full scan and isolation modes, respectively; IC_{Full} is the RawOvFtT value in the full scan mode; I_Σ is the summed ion intensity in the full scan mode; I_i is the intensity of the ion of interest and *IT* is the ion transmission.

Supporting figures

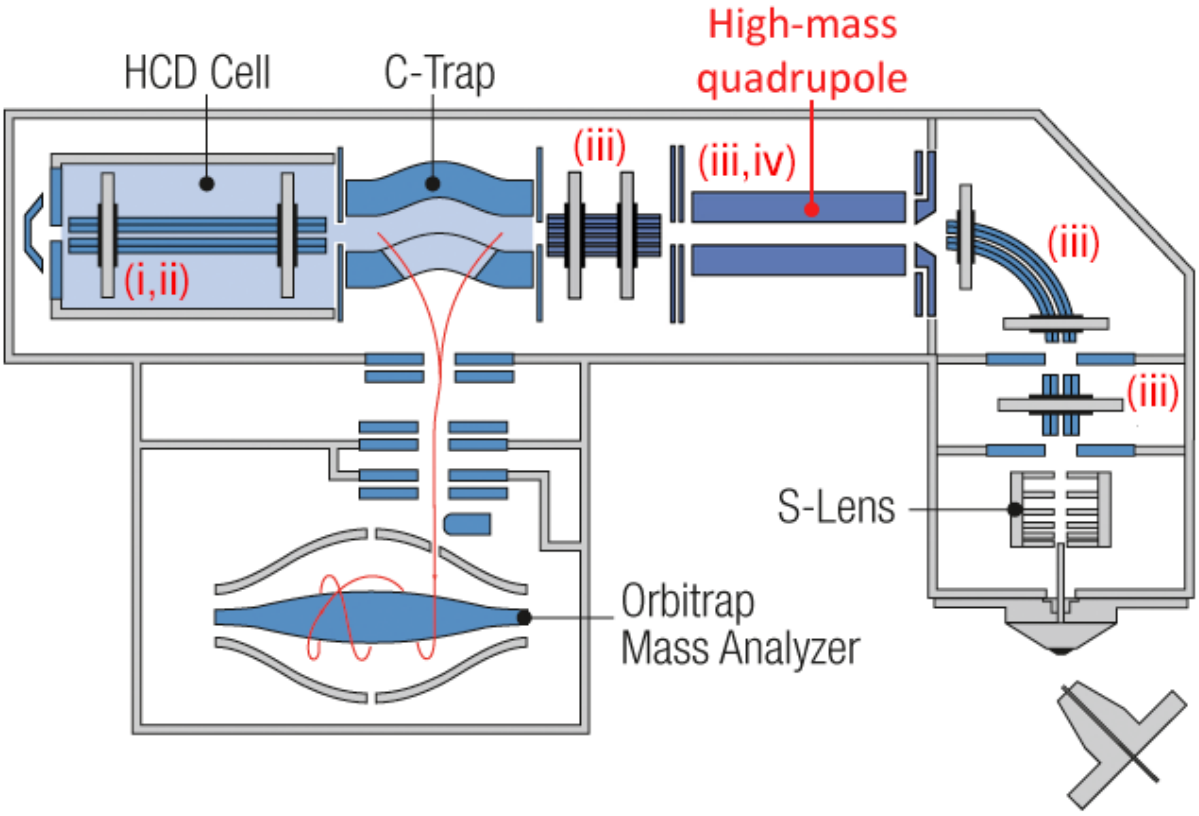

Figure S1. Schematic of the Orbitrap Exactive Plus mass-spectrometer modified for optimal transmission and detection of ions with m/z up to 50,000. The ions are trapped in the HCD cell for efficient cooling and optional collisional activation (i); dedicated gas line enables control over the pressure and the type of gas in the HCD cell (ii); RF frequencies on the transfer ion guides are lowered and manual control over the transfer optics DC offsets is enabled (iii); high-mass quadrupole with a resonance frequency of 284 kHz and a upper mass-selection limit of 20000 m/z (iv).

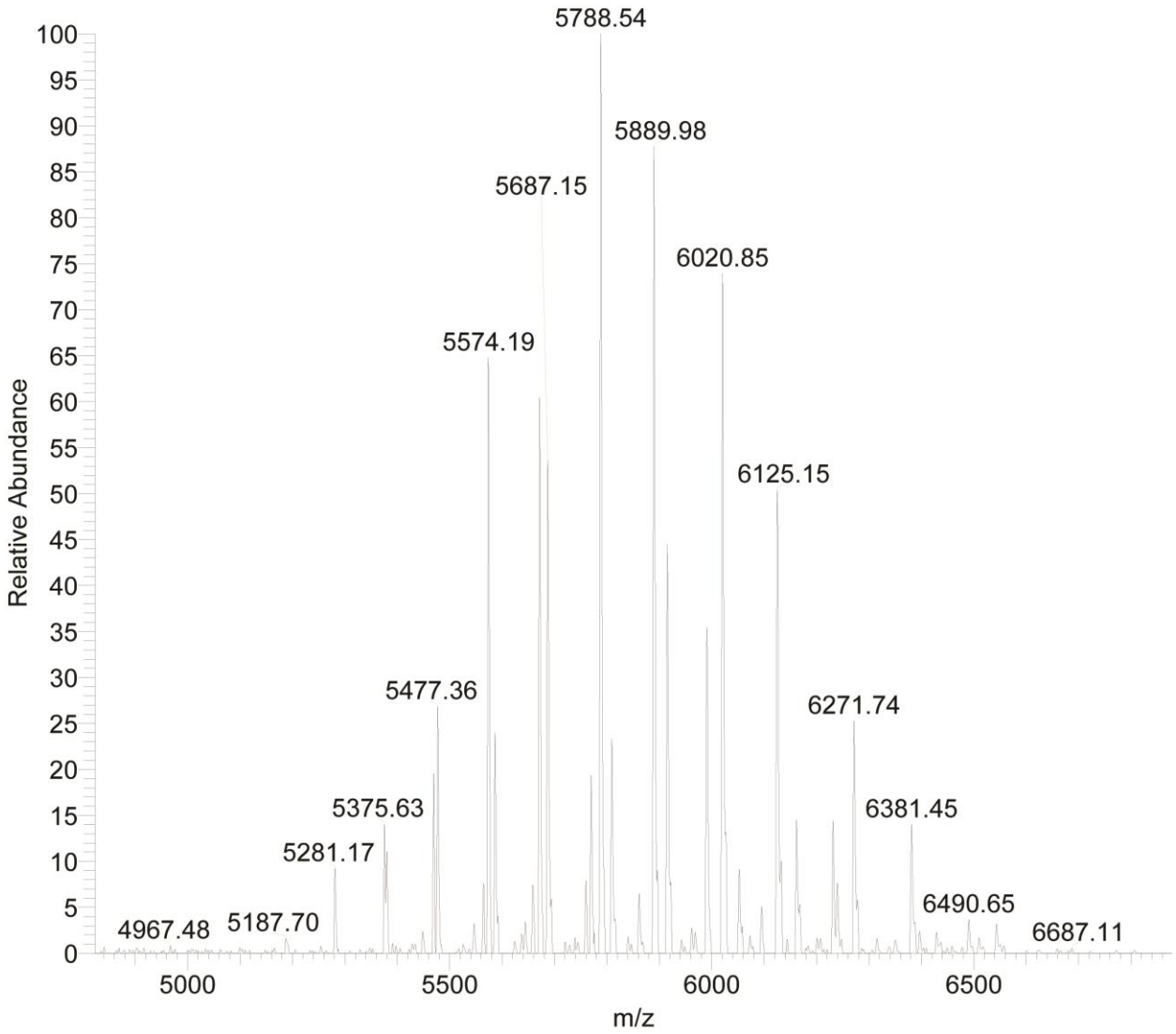

Figure S2. Full MS spectrum of partially reduced brentuximab vedotin. An average increase in mass of about 70 ppm is due to lower transmission and acceleration voltages used in order to prevent dissociation of the reduced sample, but leading to less efficient desolvation.

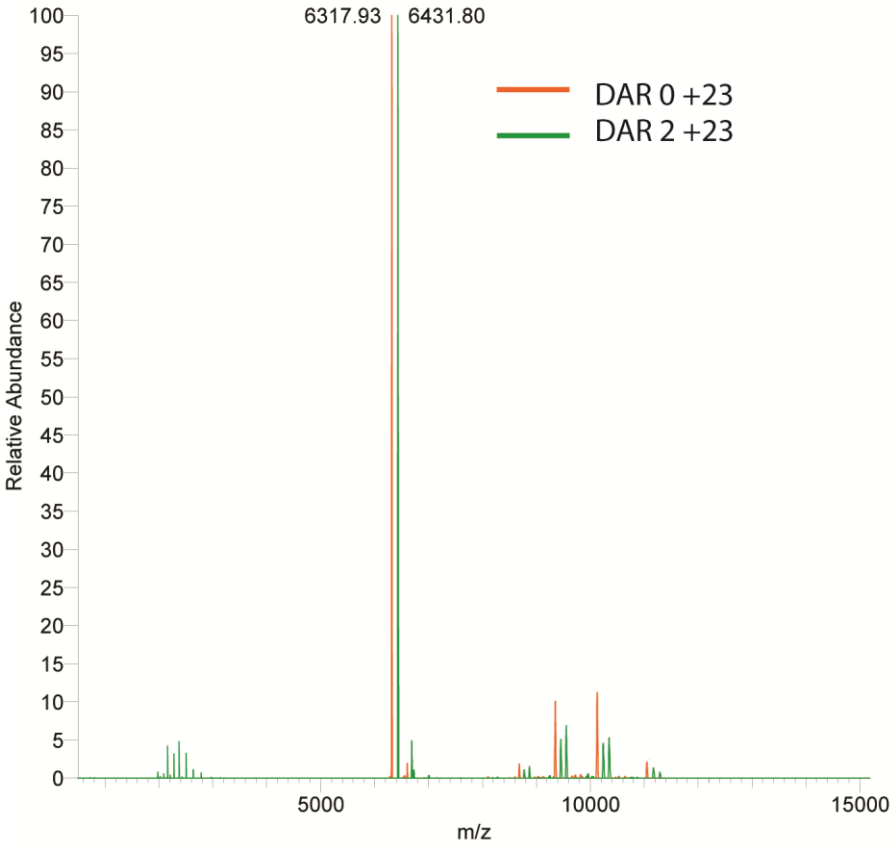

Figure S3. Fragmentation spectra of DAR0 species (+23 charge, orange) and DAR2 species (+23, green) shown on the same plot for comparison. Each spectrum combines 100 scans of 10 microscans each acquired at 17500@200 resolution. The calculated intensity ratio of parent ion relative to the fragment ions are 79.8:20.2 (DAR0) and 79.1:20:9 (DAR2).

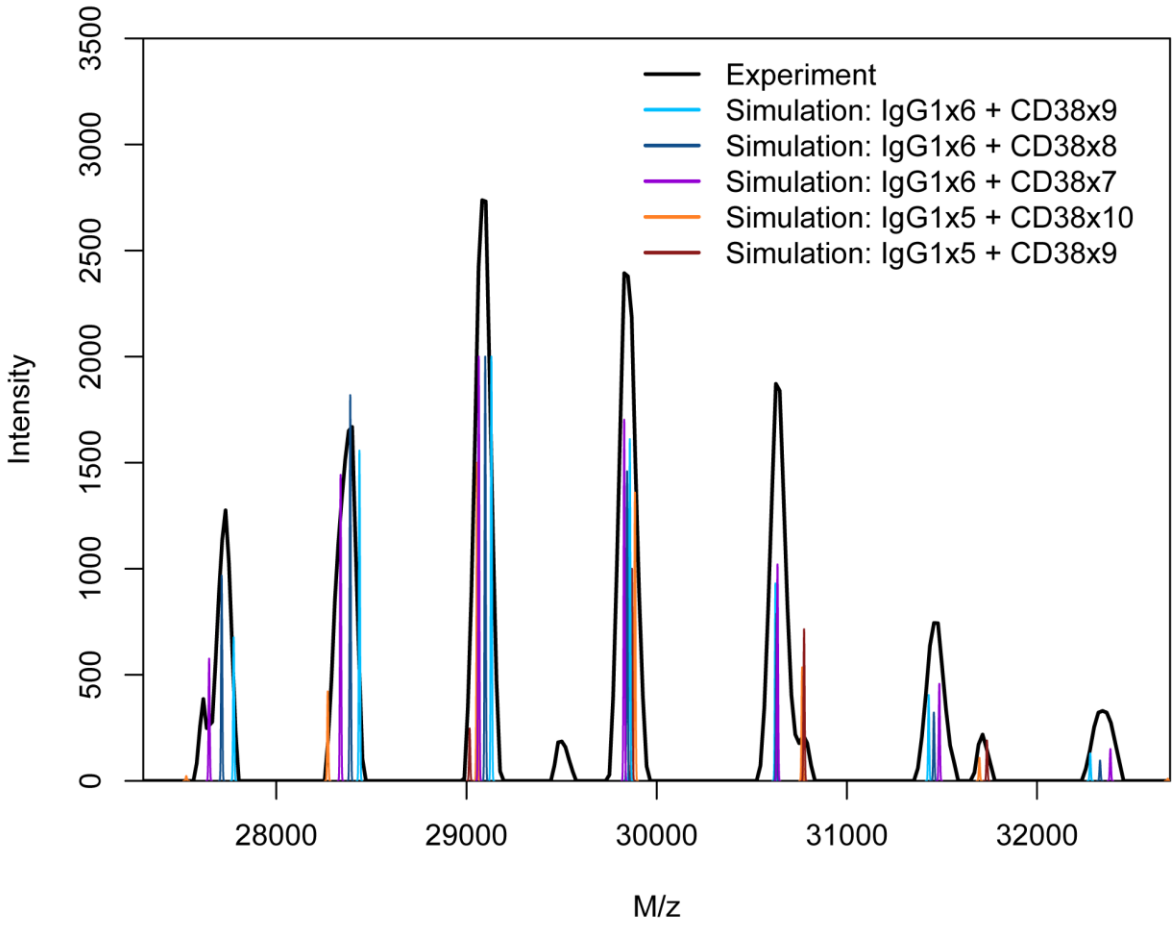

Figure S4. Tandem MS spectrum of $IgG1_6$:$CD38_{12}$ at the acceleration voltage of 200V, zoom in on 27500-32500 m/z region. Similar to the precursor ions peak envelope, the broad peaks in this region correspond to several partially overlapping species. The simulation suggests that the major peak distribution originates mainly from the loss of CD38 by the $IgG1_6$:$CD38_{10}$, $IgG1_6$:$CD38_9$ and $IgG1_6$:$CD38_8$ precursor ions. Additional peaks can be partly explained by the loss of IgG1 from $IgG1_6$:$CD38_{10}$ and $IgG1_6$:$CD38_9$ precursor ions.

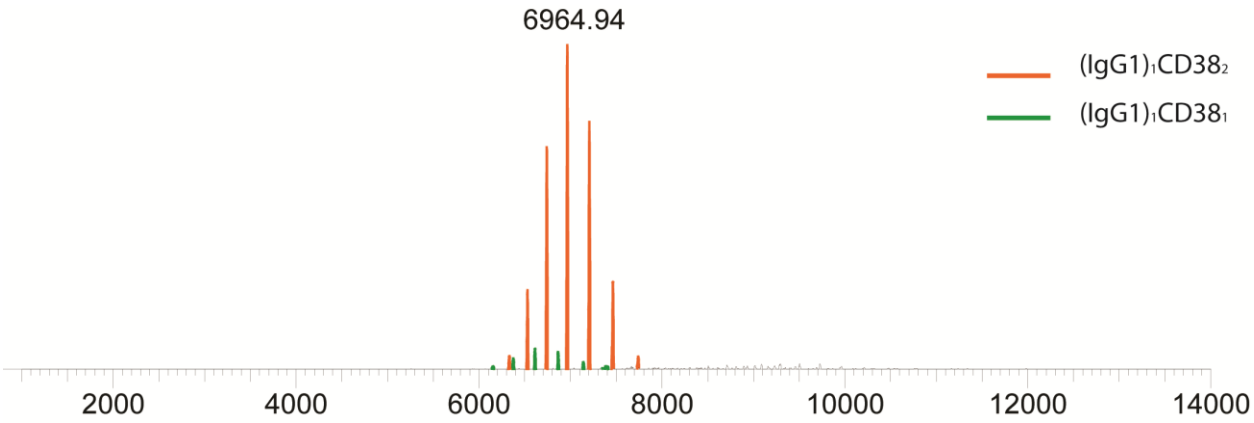

Figure S5. Native mass-spectrum of the IgG1-005:sCD38 complex acquired at a mixing ratio of 1:2.5. The relative abundances of $(IgG1)_1sCD38_2$ and $(IgG1)_1sCD38_1$ calculated from the peak intensities are 0.95 and 0.5 respectively.

Supporting tables

	Theoretical mass, Da	Experimental mass, Da	Mass Error, ppm	Mass Error, Da	Average Charge
DAR 0[a]	145190.4	145199.0±1.7	59.1	8.6	23.35±0.4
DAR 2[b]	147835.5	147836.8±1.1	8.4	1.2	23.24±0.3
DAR 4	150473.3	150472.5±1.3	5.1	0.8	23.64±0.3
DAR 6	153109.1	153107.1±1.5	13.0	2.0	24.01±0.3
DAR 8	155743.6	155745.1±1.8	9.9	1.5	24.24±0.4

Table S1. Theoretical and experimental masses of brentuximab vedotin ADC with different number of MMAE molecules.

[a]Theoretical mass of the unconjugated parent brentuximab molecule was calculated from the sequence. The modifications taken into account include heavy chain Asn297 deamidation (+ 0.98 Da) and N-terminal pyroglutamic acid formation (- 18.02 Da). The 8.6 Da discrepancy is caused most likely by the unknown PTMs.

[b]Species with higher DAR values were calculated by adding theoretical mass of vcMMAE (1318.3 Da) to the experimental mass of unconjugated brentuximab.

	Native MS		**Le et. al.**	
	$DAR2_F$	**$DAR2_H$**	**$DAR2_F$**	**$DAR2_H$**
% in ADC	23.0	1.1	27.7	2.6
% in DAR2	95.6	6.4	91.7	8.5

	Native MS		**Le et. al.**	
	$DAR6_{FFH}$	**$DAR6_{FHH}$**	**$DAR6_{FFH}$**	**$DAR6_{FHH}$**
% in ADC	1.5	22.4	0.6	10.9
% in DAR6	6.4	93.6	5.2	94.8

Table S2. Positional stoichiometry and localization of the drug molecules in the DAR2 and DAR6 species calculated from the native tandem MS spectra, compared to the values obtained by Le *et.al.* using a HIC/CE-SDS approach[28]. The "% in ADC" depicts the fraction of the isomer compared to all the species present in ADC; "% in DAR2" and "% in DAR6" represent the fraction of the isomer compared to the species with the DAR 2 and DAR6, respectively. The subscript F and H represents the isomers with the drug bound in the Fab and hinge regions, respectively.

IgG1-2F8-RGY monomer

m/z	z	mass(Da)	ΔM, ppm
5749.91	26	149471.7	274.5
5981.49	25	149512.3	3.0
6231.21	24	149525	82.5
6502.82	23	149541.9	195.0
Average mass		149512.7	
Standard deviation		25.91846	

IgG1-2F8-RGY dimer

m/z	z	mass(Da)	ΔM, ppm
7669.26	39	299062.1	88.8
7870.45	38	299039.1	165.9
8085.3	37	299119.1	101.5
8309.79	36	299116.4	92.6
8546.91	35	299106.9	60.5
Average mass		299088.7	
Standard deviation		32.21391	

IgG1-2F8-RGY trimer

m/z	z	mass(Da)	ΔM, ppm
8794.99	51	448493.5	187.9
8971.22	50	448511	148.81
9158.04	49	448695	261.2
9346.47	48	448582.6	10.6
9545.02	47	448568.9	19.7
9753.14	46	448598.4	46.0
9969.78	45	448595.1	38.6
Average mass		448577.8	
Standard deviation		61.08932	

IgG1-2F8-RGY tetramer

m/z	z	mass(Da)	ΔM, ppm
10312.61	58	598073.4	78.9
10495.15	57	598166.6	76.7
10682.47	56	598162.3	69.7
10876.93	55	598176.2	92.8
11075.38	54	598016.5	174.0
11286.45	53	598128.9	13.7
Average mass		598120.6	
Standard deviation		57.83338	

IgG1-2F8-RGY hexamer

m/z	z	mass(Da)	ΔM, ppm
11963.74	75	897205.5	109.0
12124.5	74	897139	34.9
12290.4	73	897126.2	20.6
12460.21	72	897063.1	49.6
12636.05	71	897088.6	21.3
12816.16	70	897061.2	51.8
13002.52	69	897104.9	3.1
13193.98	68	897122.6	16.6
13388.99	67	896995.3	125.2
13594.49	66	897170.3	69.8
Average mass		897107.7	
Standard deviation		56.73188	

Table S3. Peak assignment of the native mass spectrum of IgG1-2F8-RGY mixed with sCD38 at a ratio of 1:2.5. No binding of sCD38 is observed.

$IgG1_1$:$sCD38_2$

m/z	z	mass(Da)	ΔM, ppm
6153.79	35	209228.9	319.0
6341.01	34	209253.3	202.1
6541.34	33	209322.9	130.2
6752.97	32	209342.1	221.9
6977.7	31	209331	169.0
Average mass		209295.6	
Standard deviation		50.98479	

Table S4. Peak assignment of the native mass spectrum of IgG1-005-RGY complex with sCD38 mixed with sCD38 at a ratio of 1:2.5. The binding stoichiometry is 1:2 (IgG:sCD38)

First dissociation - IgG_6:$sCD38_{11}$

m/z	z	mass(Da)	ΔM, ppm
16550.61	74	1224671	144.3
16778.41	73	1224751	79.2
17010.93	72	1224715	108.5
17250.56	71	1224719	105.4
17500.16	70	1224941	76.2
17752.37	69	1224845	2.8
18013.86	68	1224874	21.7
18283.02	67	1224895	38.7
18560.84	66	1224949	82.9
18846.18	65	1224937	72.5
19140.1	64	1224902	44.5
19443.58	63	1224883	28.3
19758.53	62	1224967	97.1
20075.98	61	1224574	223.8
20419.26	60	1225096	202.2
Average mass		1224848	
Standard deviation		131.6	

First dissociation - IgG_6:$sCD38_{10}$

m/z	z	mass(Da)	ΔM, ppm
16361.92	73	1194347	105.2
16593.25	72	1194642	141.7
16824.43	71	1194464	7.8
17064.34	70	1194434	32.6
17312.37	69	1194485	9.8
17567.36	68	1194512	33.2
17828.71	67	1194457	13.6
18099.51	66	1194502	24.2
18378.19	65	1194517	37.3
18665.68	64	1194540	55.9
18962.36	63	1194566	77.8
19267.67	62	1194534	50.9
19583.94	61	1194559	72.5
19905.6	60	1194276	164.8
20243.38	59	1194300	144.3
20594.64	58	1194431	34.9
Average mass		1194473	
Standard deviation		95.3	

Second dissociation - IgG_6:$sCD38_{10}$

m/z	z	mass(Da)	ΔM, ppm
21713.96	55	1194213	217.7
22121.66	54	1194516	35.9
22537.64	53	1194442	25.8
22972.54	52	1194520	39.6
23422.4	51	1194491	15.6
23889.87	50	1194444	24.5
24378.27	49	1194486	11.2
24885.76	48	1194468	3.6
25416.46	47	1194527	45.1
25976.87	46	1194890	349.3
Average mass		1194500	
Standard deviation		156.1	

First dissociation - IgG_6:$sCD38_9$

m/z	z	mass(Da)	ΔM, ppm
16403.94	71	1164609	302.1
16639.05	70	1164664	348.0
16872.91	69	1164162	72.0
17122.61	68	1164269	18.1
17377.04	67	1164195	44.5
17639.87	66	1164165	69.0
17913.8	65	1164332	70.5
18191.56	64	1164196	43.5
18477.16	63	1163998	209.1
18773.4	62	1163889	300.6
Average mass		1164248	
Standard deviation		228.4	

Second dissociation - IgG_6:$sCD38_9$

m/z	z	mass(Da)	ΔM, ppm
21559.14	54	1164140	46.2
21964.84	53	1164084	1.9
22388	52	1164124	32.9
22825.05	51	1164027	50.9
23284.08	50	1164154	58.6
23758.71	49	1164128	36.1
24252.54	48	1164074	10.2
24769.21	47	1164106	17.3
25303.97	46	1163937	128.1
Average mass		1164086	
Standard deviation		64.2	

Second dissociation - IgG_6:$sCD38_8$

m/z	z	mass(Da)	ΔM, ppm
21803.21	52	1133715	79.9
22227.06	51	1133529	84.0
22678.61	50	1133881	226.0
23132.94	49	1133465	140.5
23617.89	48	1133611	12.0
24121.42	47	1133660	31.2
24642.53	46	1133510	100.5
Average mass		1133624	
Standard deviation		132.4	

Table S5. Peak assignment of the CID fragments of $IgG1_6$:$sCD38_{12}$ parent assembly at 150V HCD accelerating voltage.

	Relative abundance, %	
	1^{st} dissociation	2^{nd} dissociation
IgG_6:$sCD38_{11}$	51.7	
IgG_6:$sCD38_{10}$	38.3	53
IgG_6:$sCD38_9$	10	37.6
IgG_6:$sCD38_8$		9.3

Table S6. Relative abundances of CID fragments of $IgG1_6$:$sCD38_{12}$ parent assembly at 150V HCD accelerating voltage calculated from summed peak intensities after 1^{st} and second dissociation event.